LSND and MiniBooNE as guideposts to understanding the muon $g - 2$ results and the CDF II W mass measurement

Waleed Abdallah [a], Raj Gandhi [b], Samiran Roy [c],*

[a] *Department of Mathematics, Faculty of Science, Cairo University, Giza 12613, Egypt*
[b] *Harish-Chandra Research Institute (A CI of the Homi Bhabha National Institute), Chhatnag Road, Jhunsi, Allahabad 211019, India*
[c] *INFN - Sezione di Napoli, Complesso Univ. Monte S. Angelo, I-80126 Napoli, Italy*

A R T I C L E   I N F O

A B S T R A C T

In recent times, several experiments have observed results that are in significant conflict with the predictions of the Standard Model (SM). Two neutrino experiments, LSND and MiniBooNE (MB) have reported electron-like signal excesses above backgrounds. Both the Brookhaven and the Fermilab muon $g - 2$ collaborations have measured values of this parameter which, while consistent with each other, are in conflict with the SM. Recently, the CDF II collaboration has reported a precision measurement of the W-boson mass that is in strong conflict with the SM prediction. It is worthwhile to seek new physics which may underly all four anomalies. In such a quest, the neutrino experiments could play a crucial role, because once a common solution to these anomalies is sought, LSND and MB, due to their highly restrictive requirements and observed final states, help to greatly narrow the multiplicity of new physics possibilities that are otherwise open to the W mass and muon $g - 2$ discrepancies. Pursuant to this, earlier work has shown that LSND, MB and the muon $g - 2$ results can be understood in the context of a scalar extension of the SM which incorporates a second Higgs doublet and a dark sector singlet. We show that the same model leads to a contribution to the W mass which is consistent with the recent CDF II measurement. While the LSND, MB fits and the muon $g - 2$ results help determine the masses of the light scalars in the model, the calculation of the oblique parameters S and T determines the allowed mass ranges of the heavier pseudoscalar and the charged Higgs bosons as well as the effective Weinberg angle and its new range.

© 2023 The Author(s). Published by Elsevier B.V. This is an open access article under the CC BY license (http://creativecommons.org/licenses/by/4.0/). Funded by SCOAP³.

1. Introduction

The Standard Model (SM) of particle interactions has provided us with one of the most successful theories in all of physics. Its foundations were laid in the 1950s and through the early 1970s.[1] The structure of this $SU(3)_c \times SU(2)_L \times U(1)_Y$ model of strong and electro-weak interactions has been subsequently fleshed out

and embellished by the work of thousands of experimental and theoretical physicists. It has undergone rigorous and increasingly accurate testing in numerous accelerator and non-accelerator experiments over a period of about five decades. Moreover, these checks on its validity and precision have occurred over an impressively large range of energies. Recent examples of the breadth of its applicability are measurements of coherent elastic neutrino-nucleon scattering (CEνNS) by the COHERENT experiment [13], involving keV-scale nuclear recoils on the one hand and the possible detection of a 6.3 PeV Glashow resonance event by the Ice-Cube collaboration [14], on the other. In addition, this bedrock of modern-day physics has also provided very dependable predictions for expected measurements and backgrounds for a host of experiments, which has been invaluable during their planning and data-analysis stage.

Of late, however, cracks seem to have appeared in this magnificent edifice. These worrying fissures take the form of reliable measurements which deviate significantly from its predictions. Four of the most important of these are:

---

* Corresponding author.

E-mail addresses: awaleed@sci.cu.edu.eg (W. Abdallah), raj@hri.res.in (R. Gandhi), samroy@na.infn.it (S. Roy).

[1] Foundational work on the SM can be considered to have begun with work in 1954 by Yang and Mills on non-abelian gauge theories [1]. It was followed by Glashow's work on combining the weak and electromagnetic interactions [2] and the subsequent incorporation of the Higgs mechanism [3–5] by Weinberg [6] and Salam [7]. Crucial to subsequent theoretical and experimental progress was work by 't Hooft and Veltman on the regularization and renormalization of spontaneously broken gauge theories [8–10]. Finally, asymptotic freedom was shown to hold in the strong interactions by Gross, Wilczek and Politzer [11,12], rounding off about two decades of remarkable developments.

- The recent precise measurement of the W-boson mass [15], yielding

$$M_W = 80,433.5 \pm 9.4 \text{ MeV}$$

using 8.8 fb^{-1} of $\sqrt{s} = 1.96$ TeV $p\bar{p}$ collision data from the CDF II detector at the Fermilab Tevatron. This differs from the SM prediction [16] of

$$M_W^{\text{SM}} = 80,357 \pm 6 \text{ MeV}$$

at a level which amounts to a discrepancy of 7σ. We also note, however, that the CDF II measurement is in tension with the earlier measurements of M_W at LEP [17], Tevatron [18] and the LHC [19], which lead to the current world average [20] value of

$$M_W^{\text{exp}} = 80,379 \pm 12 \text{ MeV}.$$

- The recent Fermilab muon $g-2$ collaboration's precise measurement of the muon anomalous magnetic moment, $a_\mu^{\text{FNAL}} = 116592040(54) \times 10^{-11}$ [21], consistent with the prior Brookhaven $g-2$ collaboration measurement of $a_\mu^{\text{BNL}} = 116592089(63) \times 10^{-11}$ [22,23]. These measurements, when combined, differ from the SM theoretical prediction of $a_\mu^{\text{SM}} = 116591810(43) \times 10^{-11}$ [24–44] by a confidence level of 4.2σ.
- The observation of unexplained electron-like excesses in the Liquid Scintillator Neutrino Detector (LSND) [45,46] at a level of 3.8σ above known SM backgrounds.
- The observation of a similar, unexpected 4.8σ excess in electron-like events in the MiniBooNE (MB) detector [47–49].

The CDF II measurement has strengthened the case for new physics explanations, given the large deviation from the expected SM value. This has led to a very large number of proposed explanations involving highly diverse physics beyond the SM (BSM), including the two-Higgs doublet model (2HDM) with extensions [50–66], supersymmetry [67–72], triplet Higgs extensions [73–79], seesaw models [80–85], models with leptoquarks [86–89], analyses using SM effective theories (SMEFTs) [90–99], vector-like fermions [100–104], as well as other mechanisms [105–117].

Similarly, a very large number of new physics proposals for the muon $g-2$ discrepancy have been put forth. These are too numerous for us to provide individual references here, and hence the reader is referred to the reviews in [118,119] for details and a full set of references. Possible solutions arise from technicolour, supersymmetry, composite models, 2HDMs, extra dimensions, new gauge bosons, leptoquarks, Higgs triplets, vector-like leptons and very weakly interacting scalars.

The combined significance of the LSND and MB results is 6.1σ [48]. The results are backed by careful measurements and estimates of possible SM backgrounds in order to eliminate standard physics explanations. (For discussions, see e.g. [120–125] and references therein.) Many new physics explanations have been proposed for these anomalies, and for a review and references we refer the reader to [126]. An important qualitative difference between these anomalies and those observed by the muon $g-2$ and CDF II experiments is the multiplicity and tightness of constraints in the former case. This situation stems from the low energy (and hence well tested) environment at which new physics must manifest itself to explain LSND and MB, as well as the fact that the final states in the two detectors have been observed to be electron-like.[2] It also arises because their angular and en-

ergy distributions have been measured and found to be distinctive. The constraints on LSND and MB originate from oscillation experiments, requirements based on anomaly cancellation, a host of decay experiments, a variety of neutrino-nucleon neutral current measurements at both high and low energies, mixings between SM and sterile neutrinos, neutrino-electron scattering measurements, coherent neutrino-nucleon scattering, dark photon searches, beam dump experiments, near-detector measurements in long-baseline experiments, collider experiments, Higgs physics, vacuum stability requirements and electroweak precision measurements (see, for a discussion and full references [126–128]).

Additionally, we note that most proposed new physics solutions for LSND and MB involve the tree-level *in-situ* production of low mass particles and lead to a restricted number of viable proposals. In contrast, many (but not all) viable solutions to account for the muon $g-2$ and CDF II results involve new heavy particles and loop effects, allowing a large number of new physics possibilities.

There are proposals which aim to explain both the CDF II and the muon $g-2$ measurements, as in for instance [60,61,63,68,69, 83,86–88,100,101,103]. While it is not necessary, it is certainly desirable that there exist a relatively simple and natural extension of the SM which accounts for all four of these anomalies. Due to the reasons above, when seeking a common understanding of the four anomalies, LSND and MB provide a strategically superior starting point. Prior to the CDF II W-mass result, it was shown in [128] that when the SM is extended by a second Higgs doublet plus a light singlet scalar and three right-handed neutrinos, one obtains *i*) a resolution of both the LSND and MB anomalies, *ii*) a portal to the dark sector, *iii*) an agreement with the experimentally observed value of the muon $g-2$ and *iv*) an understanding of neutrino mass via a Type I seesaw, in conformity with the observed values of neutrino mass-squared differences in oscillation experiments. Further justification for the approach adopted in [128] was discussed in [126]. In this work, we show that this model, with the parameter values used to obtain *i*) through *iv*), can also account for the CDF II result on the W-boson mass, and, in the process, add further information on the heavier charged and neutral Higgs bosons constituting it.

Finally, before concluding this section, we take note of a fifth, significant discrepancy with SM predictions *i.e.* the B anomalies, measured in observables related to the charged and neutral current decays of the beauty quark, $b \rightarrow s l^+ l^-$ and $b \rightarrow c l^- \bar{\nu}_l$. In particular, they manifest themselves in the observable R_K for the former and $R(D^*)$ for the latter category of decays. (For a review and references see [129].) We do not address them in this paper. However, we note that the $R(D^*)$ anomaly is amenable to a resolution by a charged Higgs in the mass range 180 GeV $\leq m_{H^\pm} \leq$ 400 GeV, as discussed recently in [130–133]. This mass range agrees well with the one predicted by our model in this work (as shown below).

Section 2 provides a brief description of the essential elements of the model in [128] and also recapitulates the important results obtained in that paper on the LSND, MB and muon $g-2$ anomalies. Section 3 provides details of the calculation of the correction to the W mass which results from the model. Section 4 presents our results, section 5 contains a discussion and section 6 presents our conclusions.

2. Summary of the model and earlier results

Our model extends the scalar sector of the SM by augmenting it with a second Higgs doublet, *i.e.*, the widely studied 2HDM [134, 135]. Additionally, it incorporates a dark singlet real scalar $\phi_{h'}$. Three right-handed neutrinos help generate neutrino masses via the seesaw mechanism. For brevity, we have not included the neutrino part of the Lagrangian here, since it is not directly relevant to the W mass issue we address in this paper. Consequently, only

---

[2] Both detectors cannot distinguish between final-state electrons, photons or e^+e^- pairs.
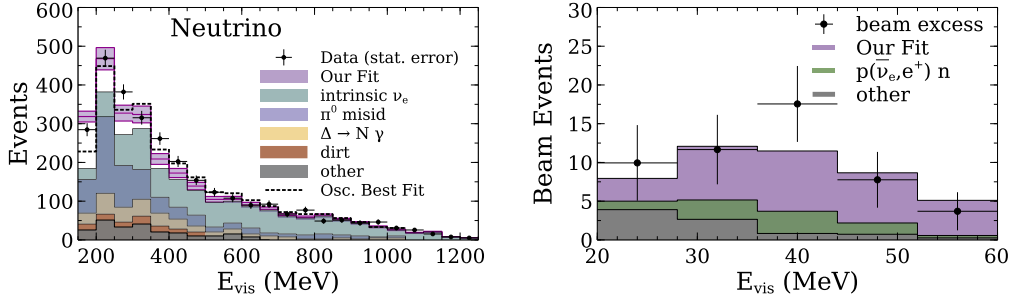
Fig. 1. Left panel: The MB electron-like events (backgrounds and signal), taken from [49], versus the visible energy E_{vis}, for neutrino beam runs. Right panel: The distribution of the LSND events versus E_{vis} [46]. The shaded purple region in both panels is the fit from our model, and other shaded regions are the backgrounds. (From [128].)

the scalar part of the Lagrangian is provided below. Full details of the model and the results it leads to can be found in [128].

With the λ_i denoting the usual set of quartic couplings, we write the scalar potential V in the Higgs basis $(\phi_h, \phi_H, \phi_{h'})$ [136, 137] as

$$
\begin{aligned}
V = &|\phi_h|^2 \left(\frac{\lambda_1}{2} |\phi_h|^2 + \lambda_3 |\phi_H|^2 + \mu_1 \right) \\
&+ |\phi_H|^2 \left(\frac{\lambda_2}{2} |\phi_H|^2 + \mu_2 \right) + \lambda_4 (\phi_H^\dagger \phi_h)(\phi_H^\dagger \phi_h) \\
&+ \phi_{h'}^2 \left(\lambda_2' \phi_{h'}^2 + \lambda_3' |\phi_h|^2 + \lambda_4' |\phi_H|^2 + m' \phi_{h'} + \mu' \right) \\
&+ \left[\phi_h^\dagger \phi_H \left(\frac{\lambda_5}{2} \phi_h^\dagger \phi_H + \lambda_6 |\phi_h|^2 + \lambda_7 |\phi_H|^2 + \lambda_5' \phi_{h'}^2 - \mu_{12} \right) \right. \\
&\left. + \phi_{h'}(m_1 |\phi_h|^2 + m_2 |\phi_H|^2 + m_{12} \phi_h^\dagger \phi_H) + h.c. \right],
\end{aligned}
\tag{1}
$$

where

$$
\phi_h = \begin{pmatrix} H_1^+ \\ \frac{v + H_1^0 + i G^0}{\sqrt{2}} \end{pmatrix} \equiv \cos\beta\, \Phi_1 + \sin\beta\, \Phi_2,
\tag{2}
$$

$$
\phi_H = \begin{pmatrix} H_2^+ \\ \frac{H_2^0 + i A^0}{\sqrt{2}} \end{pmatrix} \equiv -\sin\beta\, \Phi_1 + \cos\beta\, \Phi_2,
\tag{3}
$$

$$
\phi_{h'} = H_3^0 / \sqrt{2}.
\tag{4}
$$

With v, v_i denoting vacuum expectation values (vevs), so that $v^2 = v_1^2 + v_2^2 \simeq (246 \text{ GeV})^2$ and $\tan\beta = v_2/v_1$, where $\langle \Phi_i \rangle = v_i/\sqrt{2}$, $\langle \phi_h \rangle = v$ while $\langle \phi_H \rangle = 0 = \langle \phi_{h'} \rangle$. Here, H_1^+, G^0 are the Goldstone bosons which give the gauge bosons mass after the spontaneous breaking of electroweak symmetry. In the basis (H_1^0, H_2^0, H_3^0), the neutral CP-even Higgs mass matrix is given by

$$
m_{\mathcal{H}}^2 = \begin{pmatrix} \lambda_1 v^2 & \lambda_6 v^2 & 0 \\ \lambda_6 v^2 & \mu_H & m_{12} v/\sqrt{2} \\ 0 & m_{12} v/\sqrt{2} & \mu_{h'} \end{pmatrix},
\tag{5}
$$

where $\mu_H = \mu_2 + (\lambda_3 + \lambda_4 + \lambda_5) v^2/2$ and $\mu_{h'} = \mu' + \lambda_3' v^2/2$. Minimization of the scalar potential V yields the conditions,

$$
m_1 = 0, \quad \mu_1 = -\frac{1}{2} \lambda_1 v^2, \quad \mu_{12} = \frac{1}{2} \lambda_6 v^2.
\tag{6}
$$

In the alignment limit (i.e., $\lambda_6 \simeq 0$), we diagonalize $m_{\mathcal{H}}^2$ in Eq. (5) by $Z^{\mathcal{H}} m_{\mathcal{H}}^2 (Z^{\mathcal{H}})^T = (m_{\mathcal{H}}^2)^{\text{diag}}$, with

$$
Z^{\mathcal{H}} = \begin{pmatrix} 1 & 0 & 0 \\ 0 & \cos\delta & -\sin\delta \\ 0 & \sin\delta & \cos\delta \end{pmatrix}.
\tag{7}
$$

Here

Table 1
Benchmark point used for event generation in LSND, MB and for calculating the muon $g-2$.

m_{N_1}	m_{N_2}	m_{N_3}	$y_u^{h'(H)} \times 10^6$	$y_{e(\mu)}^{h'} \times 10^4$	$y_{e(\mu)}^H \times 10^4$
85 MeV	130 MeV	10 GeV	0.8(8)	0.23(1.6)	2.29(15.9)
$m_{h'}$	m_H	$\sin\delta$	$y_d^{h'(H)} \times 10^6$	$y_{\nu_{i2}}^{h'(H)} \times 10^3$	$\lambda_{N_{12}}^{h'(H)} \times 10^3$
17 MeV	750 MeV	0.1	0.8(8)	1.25(12.4)	74.6(−7.5)

$$
\tan 2\delta = \frac{\sqrt{2}\, m_{12} v}{\mu_{h'} - \mu_H}, \qquad H_i^0 = \sum_j Z_{ji}^{\mathcal{H}} h_j,
\tag{8}
$$

and i) δ is the scalar mixing angle between the gauge eigenstates (H_2^0, H_3^0) and the mass eigenstates (H, h'), ii) $(h_1, h_2, h_3) = (h, H, h')$ are the mass eigenstates, iii) $H_1^0 \approx h$ is the SM-like Higgs, $m_h^2 \simeq \lambda_1 v^2$ and iv) $m_{12} < 0$ so as to obtain $m_H^2 \geq m_{h'}^2$. Therefore, the extra CP-even physical Higgs states (H, h') have masses given by

$$
m_{H,h'}^2 \simeq \frac{1}{2} \left[\mu_H + \mu_{h'} \pm \sqrt{(\mu_H - \mu_{h'})^2 + 2 m_{12}^2 v^2} \right].
\tag{9}
$$

Finally, the CP-odd Higgs mass is given by

$$
m_A^2 = m_{H^\pm}^2 + (\lambda_4 - \lambda_5) v^2/2,
\tag{10}
$$

and the charged Higgs mass is given by

$$
m_{H^\pm}^2 = \mu_2 + \lambda_3 v^2/2.
\tag{11}
$$

After making a convenient basis rotation, the coupling strengths of the scalars (h', H) with fermions (leptons and quarks)[3] are $(y_f^{h'}, y_f^H)$. Similar considerations apply to neutrinos, where the coupling strengths of the light scalars (h', H) for vertices connecting active and sterile neutrinos are $(y_{\nu_{ij}}^{h'}, y_{\nu_{ij}}^H)$ while the couplings of the scalars (h', H) to the sterile states are $(\lambda_{N_{ij}}^{h'}, \lambda_{N_{ij}}^H)$. Our choice of benchmarks for the fits shown in Fig. 1 is such that the values are compatible with experimental values of global fits of neutrino mass differences, as shown in [128]. In Fig. 1, taken from this reference, we show our results for the fits in MB (left panel) and LSND (right panel). Table 1 collects the relevant benchmark parameters associated with the fits. The masses of the three right-handed neutrinos N_i are also shown, since besides playing a role in giving the SM neutrinos a mass, they also participate in the interaction in LSND and MB responsible for the observed final state. This interaction involves the production of N_2, which decays to N_1 and h'. The latter then produces an $e^+ e^-$ pair which constitutes the electron-like signal.

---

[3] In using these to compute the muon $g-2$ contribution, we have assumed diagonal couplings to avoid FCNCs. However, under certain assumptions, off-diagonal couplings can be used to obtain this result, e.g., as in [57].

It is worth mentioning that our benchmark in Table 1 comfortably accommodates the observed value of the muon $g - 2$, where both h' and H contribute at one-loop level to the value of this parameter. The contribution of H is significantly higher for small values of $|\sin\delta|(\lesssim 0.2)$ while that of h' is around 17% for our benchmark point, as shown in Table 1.

Prior to concluding this section, we note that our approach here and in [128] has been to find the simplest model (in the sense of Occam's razor) that provides an understanding of the anomalies while still respecting known constraints. It is completely possible that the elements of the model presented here are part of a broader new physics structure. For instance, the singlet $\phi_{h'}$ could be part of a larger dark scalar multiplet. Its mass could receive contributions from the presence of a vev not considered here, as opposed to arising via a mixing with the doublet scalars. It could also have both scalar as well as pseudoscalar couplings to the SM fermions. Additionally, the general 2HDM allows for a richer CP violating structure, unlike the implicit CP conserving assumptions made in our model. Exploring the feasibility and the consequences of these possibilities and their impact on the proposed solutions to the anomalies would undoubtedly be interesting, but is outside the scope of this work.

In the next section, we calculate the contribution to the mass of the W-boson from this model.

3. Calculation of the contribution to the W mass in the model

The W-boson mass can be calculated in the SM using the measured input parameters $\{\alpha_{\mathrm{em}}, G_F, M_Z\}$ which have been accurately determined empirically [20]. Their central values are

$$
\begin{aligned}
\alpha_{\mathrm{em}}^{-1} &= 137.036, \\
G_F &= 1.1663787 \times 10^{-5}~\mathrm{GeV}^{-2}, \\
M_Z &= 91.1876~\mathrm{GeV}.
\end{aligned} \tag{12}
$$

Given these values, one may calculate the W mass using the relation [138],

$$
M_W^2 \left(1 - \frac{M_W^2}{M_Z^2} \right) = \frac{\pi \alpha_{\mathrm{em}}}{\sqrt{2} G_F} (1 + \Delta r). \tag{13}
$$

In the above equation, Δr represents higher order contributions, which arise in the SM (or its new physics extensions). Here M_W and M_Z are the renormalized masses in the on-shell scheme. One then obtains

$$
M_W^2 = \frac{M_Z^2}{2} \left[1 + \sqrt{1 - \frac{4\pi \alpha_{\mathrm{em}}}{\sqrt{2} G_F M_Z^2} (1 + \Delta r(M_W^2))} \right]. \tag{14}
$$

The additional radiative contribution Δr can be expressed as [138]

$$
\Delta r = \Delta\alpha_{\mathrm{em}} - \frac{c_W^2}{s_W^2} \delta\rho + \Delta r_{\mathrm{rem}}, \tag{15}
$$

where $c_W = \cos\theta_W$, $s_W = \sin\theta_W$ and θ_W is the Weinberg angle. The dominant contribution to Δr is from two sources: $\Delta\alpha_{\mathrm{em}}$ is a QED correction, reflecting the evolution of the fine structure coupling from $q^2 = 0$ to $q^2 = M_Z^2$ and $\delta\rho$ reflects the vacuum polarisation contributions to the ρ parameter, whose zeroth value in the SM ($\delta\rho = 0$) is

$$
\rho = \frac{M_W^2}{M_Z^2 c_W^2} = 1. \tag{16}
$$

In the SM, such radiative contributions are largely due to the top and bottom quark loops. Since Δr is a function of M_W, Eq. (14) must be solved iteratively.

The renormalization correction to the fine structure constant $\Delta\alpha_{\mathrm{em}}$ is dominated by light fermions, and is

$$
\begin{aligned}
\Delta\alpha_{\mathrm{em}} &= \frac{\alpha_{\mathrm{em}}(M_Z^2) - \alpha_{\mathrm{em}}}{\alpha_{\mathrm{em}}} \\
&= -\frac{\alpha_{\mathrm{em}}}{3\pi} \sum_{m_f < M_Z} Q_f^2 \left[\frac{5}{3} - \ln\left(\frac{M_Z^2}{m_f^2}\right) \right] \\
&= 0.05943 \pm 0.00011,
\end{aligned} \tag{17}
$$

where $\alpha_{\mathrm{em}}(M_Z^2) = 1/127.935$. $\Delta r^{[\delta\rho]} \equiv -(c_W^2/s_W^2)\delta\rho$ supplies the oblique corrections [139], while the final term, Δr_{rem} incorporates contributions from box and vertex diagram diagrams in the SM [140]. With the input parameter values given in Eq. (12) and in addition $s_W^2 = 0.2315$, $m_t = 172.76$ GeV, $m_h = 125.25$ GeV, one finds $\Delta r^{\mathrm{SM}} = \Delta\alpha_{\mathrm{em}} + \Delta r_{\mathrm{rem}} = 0.038$, and thus from an iterative solution of Eq. (14), $M_W = 80.3564$ GeV. This is 7σ and 76 MeV below the CDF II central value reported recently [15].

Any new physics which seeks to resolve this discrepancy must generate a Δr which would lead to $M_W = 80.433$ GeV, the central value of the CDF II measurement. In our model, the singlet contribution is expected to be small ($\mathcal{O}(\sim 1~\mathrm{MeV})$), as shown in [109], since both its mass and its mixing with the other neutral Higgs states are small. We thus focus on calculating the correction due to the loop contributions of the additional scalars in the doublet circulating in the W-boson self-energy diagram, since these dominate the correction. This dominance arises because unlike the SM, the scalar potential in the 2HDM does not respect custodial $SU(2)_{L+R}$ symmetry, and large corrections to the ρ parameter are possible from the additional scalar fields ($H, H^{\pm}, A$). In particular, they are proportional to the mass-squared splittings among scalars of different isospin, as apparent in Eq. (20) below.

Prior to the CDF II results, corrections to the W mass for the 2HDM have been addressed in a number of papers [140–155]. In general, the radiative correction depends on the following parameters:

$$
\Delta r = \Delta r(e, M_W, M_Z, m_f; m_{H^i}, \sin\alpha, \tan\beta, \lambda_5), \tag{18}
$$

where $H^i = h, H, H^{\pm}, A$. $\sin\alpha$ is representative of the mixing between the two neutral CP-even scalars, h, H. In the alignment limit for our model, $\sin(\beta - \alpha) \simeq 1$ and $\lambda_6 \simeq 0$. In general, the corrections of new scalars to the W-boson mass can be conveniently expressed in term of the oblique parameters S, T, and U [139,156,157], i.e.,

$$
\Delta M_W^2 = \frac{\alpha_{\mathrm{em}} c_W^2 M_Z^2}{c_W^2 - s_W^2} \left[-\frac{S}{2} + c_W^2 T + \frac{c_W^2 - s_W^2}{4 s_W^2} U \right]. \tag{19}
$$

Here $\Delta M_W^2 = M_W^2 - (M_W^{\mathrm{SM}})^2$. In an effective field theory framework, the contribution from U originates in dimension eight operators, and is consequently very small for most extensions to the SM. We thus assume $U \simeq 0$, and consider only the corrections from T (dominant) and S (subdominant) in what follows.

The dominant 2HDM contribution, in terms of a modification of the ρ parameter due to an oblique correction induced by the T parameter, calculated in the 't Hooft-Feynman gauge and denoted by $\delta\rho_{2\mathrm{HDM}}$ is [140]

$$
\begin{aligned}
\delta\rho_{2\mathrm{HDM}} = \frac{\alpha_{\mathrm{em}}}{16\pi s_W^2 M_W^2} \Bigg\{ &\cos^2(\beta - \alpha) \Big[F(m_h^2, m_{H^{\pm}}^2) \\
&- F(m_h^2, m_A^2) \Big] + F(m_A^2, m_{H^{\pm}}^2) \\
&+ \sin^2(\beta - \alpha) \Big[F(m_H^2, m_{H^{\pm}}^2) - F(m_H^2, m_A^2) \Big]
\end{aligned}
$$

$$- 3\cos^2(\beta - \alpha)\left[F(m_H^2, M_W^2) + F(m_h^2, M_Z^2)\right.$$

$$\left. - F(m_H^2, M_Z^2) - F(m_h^2, M_W^2)\right]\Bigg\}, \tag{20}$$

where the function $F(a, b)$ is defined as follows

$$F(a, b) = F(b, a) = \begin{cases} \frac{a+b}{2} - \frac{ab}{a-b}\log(\frac{a}{b}) & a \neq b \\ 0 & a = b \end{cases}. \tag{21}$$

We next approximate the full $\delta\rho$ in Eq. (15) by $\delta\rho \approx \delta\rho_{2\text{HDM}} = T\alpha_{em}(M_Z^2)$. In the alignment limit ($\alpha = \beta - \pi/2$), using Eq. (20), this allows us to write

$$T = \frac{1}{16\pi^2\alpha_{\text{em}}(M_Z^2)v^2}\left\{F(m_A^2, m_{H^\pm}^2) + F(m_H^2, m_{H^\pm}^2)\right.$$

$$\left. - F(m_H^2, m_A^2)\right\}. \tag{22}$$

In Eq. (22) above, $v^2 = (246\text{ GeV})^2 = M_W^2 s_W^2 \alpha_{\text{em}}^{-1}/\pi$.

Additionally, the contribution from the S parameter to the W mass, from Eq. (19) is,

$$\Delta M_W \simeq -\frac{M_W \alpha_{\text{em}}(M_Z^2)S}{4(c_W^2 - s_W^2)}, \tag{23}$$

where S in terms of the scalars in our model and in the alignment limit is [158]

$$S = \frac{1}{2\pi}\int\limits_0^1 dx\, x(1-x)\ln\left(\frac{xm_H^2 + (1-x)m_A^2}{m_{H^\pm}^2}\right). \tag{24}$$

We have used Eqs. (20)-(22) to calculate T, and Eq. (24) to determine S in our model. Finally, these values have been used along with Eq. (19) to calculate the mass correction. In addition to the W mass, changes in the oblique parameters also affect the effective weak mixing angle, $\sin^2\theta_{\text{eff}}$, which has been measured in several experiments [159]. The change (from the SM value) induced is given by [139]:

$$\Delta\sin^2\theta_{\text{eff}} = \frac{\alpha_{\text{em}}(M_Z^2)}{c_W^2 - s_W^2}\left[\frac{1}{4}S - s_W^2 c_W^2 T\right]. \tag{25}$$

We now proceed to present, (in the next section) results of the changes in the range of S, T and $\sin^2\theta_{\text{eff}}$ as a consequence of the CDF II correction to M_W in our model, using the formalism above. Where necessary, all values of the parameters used below are in accordance with the benchmark values specified in Table 1.

4. Results

Several recent papers have focussed on the corrections to the W mass resulting from various types of 2HDM post the CDF II measurement [50–64,153,160–162]. As is apparent from Eq. (20), the mass correction is governed by mass splittings among the scalars H, $H^\pm$ and A. Several papers have derived constraints which limit the size of these splittings and the scalar masses [55,64,161,163]. Such bounds utilize the following considerations [164]:

- the boundedness of the 2HDM potential from below [135,165],
- vacuum stability of the potential [135,166],
- high energy perturbative unitarity of the amplitudes for scalar-vector, vector-vector and scalar-scalar scattering [164,167–170],
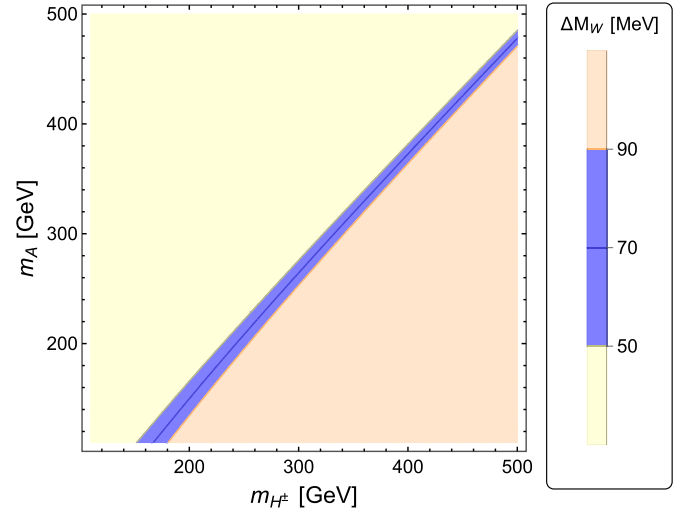

Fig. 2. Variation of ΔM_W in the $m_A - m_{H^\pm}$ plane. The blue band shows the values of m_A and $m_{H^\pm}$ in our model which lead to corrections to M_W in the range $50 - 90$ MeV. The solid blue line within the band corresponds to $\Delta M_W = 70$ MeV.

- imposition of perturbativity on the Higgs quartic couplings, λ_i, [135,171],
- bounds from LEP, LHC, electroweak precision data and FCNC processes [163,171–177].

In accordance with our aim in this paper, we focus on interpreting these bounds in the context of our model, *i.e.* for the case where the second CP-even neutral boson, H, is much lighter than the SM Higgs h, which, in turn, is lighter than the pseudoscalar A and the $H^\pm$. Applying the considerations above as discussed in [55,64,161, 163] to our model, we note that the lower bound on $m_{H^\pm}$ and m_A is $\simeq 110$ GeV, and the upper bounds on these masses may be conservatively assumed to be $\simeq 500$ GeV. Our results below also reflect the fact that $m_H \simeq 750$ MeV (see Table 1, set by fits to LSND and MB) leading to $m_{H^\pm} - m_H \approx m_{H^\pm}$ and $m_A - m_H \approx m_A$.

While all points shown in the coloured regions of Fig. 2 are compatible with our model, rigid restrictions on allowed values arise when agreement with the CDF II results is demanded. As mentioned earlier, the CDF II measurement and the one-loop corrected SM value differ by $\simeq 76$ MeV. Fig. 2 shows the blue band of values for m_A and $m_{H^\pm}$ satisfying $\Delta M_W \in [50, 90]$ MeV. The solid blue line denotes values which yield a mass difference, ΔM_W, of 70 MeV. We note that for all points in this region, $m_{H^\pm} > m_A$, and the mass differences are of the order of a couple of tens of GeV to 60 GeV.

Fig. 3 shows the possible range of S, T values when $m_{H^\pm}$ and m_A are varied in the range 110 GeV to 500 GeV. Fig. 4 plots these parameters along with the difference between the masses of the charged Higgs and the pseudo-scalar. In both figures, a) $m_H = 750$ MeV, and b) the black bands depict the region selected by the CDF measurement of the W mass, while the red band shows the corresponding region for the PDG values. The latter plot identifies the mass difference $(m_{H^\pm} - m_A)$ as positive for the CDF results, and ranging between approximately 20 GeV to 60 GeV. This differs from a more general treatment [56] aimed at determining the allowed range of S, T and mass differences between these scalars, where both a broader range as well as positive and negative values for the difference $(m_{H^\pm} - m_A)$ are possible both for CDF as well as the PDG M_W mass values.

As mentioned earlier (in the context of Fig. 2), the entire region of the $m_A - m_{H^\pm}$ shown in Fig. 5 is accessible via our model. However, changes in the oblique parameters such as those induced while seeking to explain the CDF II result modify the parameter
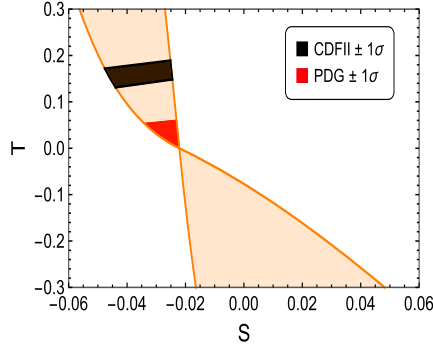
Fig. 3. Regions allowed by our model in the S and T plane. The black band shows the 1σ region selected by the M_W measurement of the CDF II experiment ($M_W = 80.4335 \pm 0.0094$ GeV) and the red band shows PDG data ($M_W = 80.379 \pm 0.012$ GeV) [20].
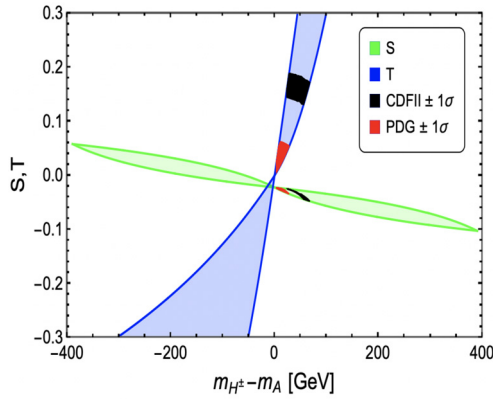

Fig. 4. The range of $m_{H^\pm} - m_A$ identified by the 1σ allowed region for M_W measurement by the CDF II experiment ($M_W = 80.4335 \pm 0.0094$ GeV) in our model (black regions, with $m_{H^\pm} - m_A \in [24, 68]$ GeV) while the red regions (with $m_{H^\pm} - m_A \in [4, 28]$ GeV) show PDG data ($M_W = 80.379 \pm 0.012$ GeV) [20].
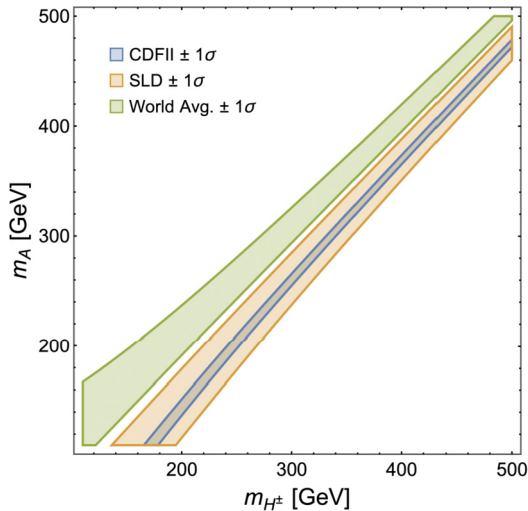

Fig. 5. The orange and green regions show, (in the $m_A - m_{H^\pm}$ plane) the 1σ allowed regions which lead to values compatible with experiment for $\sin^2 \theta_{eff}$ in our model. They correspond to the SLD measurement ($0.2307 \leq \sin^2 \theta_{eff} \leq 0.23125$) (orange band) and the world average ($0.23135 \leq \sin^2 \theta_{eff} \leq 0.2317$) (green band). The grey band shows the 1σ allowed region for M_W measurement by the CDF II experiment ($M_W = 80.4335 \pm 0.0094$ GeV) in our model.

$\sin^2 \theta_{eff}$ Eq. (25). Several measurements [159] of this parameter have been carried out. The region allowed by the world average is shown by the green band. On the other hand, measurements of $\sin^2 \theta_{eff}$ by the SLD experiment alone yield the region depicted by the orange band. Finally, the grey band in Fig. 5 (which lies entirely within the orange SLD band) shows a region yielding a correction to the W mass which ensures compatibility with CDF II. We thus note that values of $\sin^2 \theta_{eff}$ in our model which ensure the required W mass correction are in tension with the world average values, but compatible with SLD. It is important to stress, however, that the above mentioned bands are all approximately $\sim 1\sigma$, hence it is not advisable to draw any firm conclusions based on our remarks here, besides noting the fact that they are suggestive and will be clarified when more measurements are made in the future.

Our aim in this section has been to obtain a reliable estimate of the W mass correction for the model of section 2. A more rigorous calculation, as in [178], would, besides all known SM higher order corrections and the one-loop new physics effects, take into account two-loop effects of the new scalars in the model, since they are also expected to be sensitive to the mass splittings considered here. In addition, such a calculation would include the effects of the singlet scalar in our model, and not neglect its (small) mixings with the SM scalar doublets, as we have done here.

5. Discussion

A large variety of new physics proposals exist for each of the four well-established discrepancies that have been pointed to in this paper, *i.e. i*) the CDF II W mass measurement, *ii*) the muon $g - 2$ results from BNL and Fermilab, *iii*) the LSND electron-like excess and *iv*) the MB electron-like excess. Each of the anomalies has a significance level that demands attention and each is a serious contender for a signal of physics beyond the SM. It is possible that each anomaly has its own distinct solution in new physics, not overlapping with the others. On the other hand, it is reasonable to seek a simple, common BSM solution to these discrepancies.

Towards this end, we have noted that there is a qualitative difference between (*i*) and (*ii*) on the one hand, and (*iii*) and (*iv*) on the other. The W mass and the muon $g - 2$ anomalies result from precision measurements and, if connected to new physics, are likely (but not certainly) due to higher order loop effects involving new particles and interactions. The LSND and MB observations, though anomalous, involve observed final states in detectors. While for both these experiments, the final states could be either electrons, photons or $e^+ e^-$ pairs (given the inability of the two detectors to distinguish between these possibilities), this still limits the number of new physics possibilities compared to the W mass and the muon $g - 2$ anomalies. Further restrictions on proposed solutions for the CDF II results are provided by the requirement that the observed angular and energy distributions for both LSND and MB experiments must be fit by the new physics.

Additionally, since the W mass correction as calculated here depends crucially on (the high mass) charged and pseudo-scalar Higgs bosons of the 2HDM, it is useful to point out how we are actually led to this model by our effort to resolve LSND and MB. If in attempting to resolve these low energy anomalies we were to extend the SM with a singlet scalar then the coupling with other fermions would necessarily scale as $\sin \theta \, m_f / v$ (as *e.g.* in Eq. (2) of [179]). However, the constraints on such mixing with the SM Higgs are very tight (as shown in Fig. 8 of [179]). On the other hand, to explain LSND and MB, we need substantial couplings of the scalar mediators with electrons and up and down quarks, as shown in Table 1. The choice of a second Higgs doublet with a

dark scalar[4] allows us to avoid the stringent constraints mentioned above and use couplings which have sufficient strength to generate the strong excess of events seen at these detectors. One doublet obtains a vev $\simeq 246$ GeV, while the second one does not acquire a vev (as mentioned in the text related to Eqs. (2) and (3)). This alignment makes the fermion couplings to the scalar H arbitrary, and there is no m_f/v dependence. Once we induct a second Higgs doublet, we automatically have the charged Higgs and a pseudo scalar that helps to explain the CDF II measurements.

Consequently, due to the reasons discussed above, in attempts to find a common resolution, the LSND and MB anomalies provide a superior starting point that can usefully narrow the solution space considerably for the other two anomalies.

Finally, we briefly dwell on future tests of the model. An important upcoming test will be provided by the MicroBooNE experiment [180]. As part of its recent efforts [125,181–184] to pin down the origin of the excess seen in MB, it will search for the presence of e^+e^- pairs in the final state, which are an important prediction of the model presented here. Similar searches can be conducted by the Fermilab SBN program [185], including searches for the heavy neutral leptons that are part of the model. Invariant mass measurements for the produced pairs in these detectors would help pin down the mass of the h'. We also note that the masses of h' and H are close to current bounds from electron beam-dump experiments like E141 [186] (for h') and BaBar [187] (for H). This makes it possible for HPS [188] to search for h' and Belle-II [189] to search for H. Several upcoming experiments, including DUNE (see, for a discussion, *e.g.* [190–193]) will be able to search for the heavy neutral leptons in the model. The heavier scalars in the model can be searched for by the LHC. As an example, the rare (in the SM) process $pp \to t\bar{t}t\bar{t}$ is sensitive to the presence of additional scalars and pseudoscalars, via both on-shell (when the scalar mass is $> 2m_t$) and off-shell (when it is $< 2m_t$) contributions [194].

6. Conclusions

In conclusion, earlier work [126,128], summarised here, has shown that a 2HDM with a light singlet scalar and three right-handed neutrinos provides very good fits to LSND and MB data. It can also account for the measured muon $g - 2$ value and global data on neutrino mass squared differences. In this work we have shown that the model is also capable of providing a correction to the mass of the W-boson that brings it in conformity with the recent CDF II result. While remaining natural and economical, the 2HDM contains enough elements so that both LSND and MB, which are primarily effects at low (MeV-GeV) energies can be bridged and connected with the CDF II result, which requires large mass splittings and heavier scalars (few hundred GeV). We have stressed how we are led to the choice of this model by low energy results. Some salient features which distinguish it from other 2HDM extensions which address the W mass difference are i) m_A is always lower in mass than $m_{H^\pm}$; ii) Both masses are constrained to be below ~ 500 GeV, and the difference is constrained to lie between approximately ~ 20 GeV and ~ 60 GeV; iii) In addition, the second CP-even scalar (H) is much lower in mass compared to the SM Higgs (h) as well as the pseudoscalar (A) and charged Higgs ($H^\pm$) masses.

The solution of the anomalies (ii) to (iv) (as numbered in the previous section) helps obtain reference mass values for the two additional CP-even scalars in the model, $m_{h'} \simeq 17$ MeV, which is very nearly a singlet, and $m_H \simeq 750$ MeV, which is a member of the second doublet. The third CP-even scalar is very closely aligned

to the SM Higgs in mass and couplings. Addressing the CDF II anomaly provides additional mass information on the other (heavier) scalars in the model, *i.e.* the pseudoscalar A and the charged Higgs $H^\pm$. The solution space picked out demands that $m_{H^\pm} > m_A$, with masses of both below 500 GeV, and a mass difference between them of 20 GeV to 60 GeV. Finally, we note that these results pertaining to our model are in consonance and agreement with recent work seeking to understand the W mass result within the context of 2HDMs in a more general setting [50–64,153].

It is hoped that the considerations in this work help narrow the search for new physics by pointing to a candidate model which is both a simple and natural extension of the SM, as well as being one that provides a possible explanation for important outstanding anomalies.

Declaration of competing interest

The authors declare that they have no known competing financial interests or personal relationships that could have appeared to influence the work reported in this paper.

Data availability

Data will be made available on request.

Acknowledgements

References

[1] C.-N. Yang, R.L. Mills, Phys. Rev. 96 (1954) 191.
[2] S.L. Glashow, Nucl. Phys. 22 (1961) 579.
[3] F. Englert, R. Brout, Phys. Rev. Lett. 13 (1964) 321.
[4] P.W. Higgs, Phys. Rev. Lett. 13 (1964) 508.
[5] G.S. Guralnik, C.R. Hagen, T.W.B. Kibble, Phys. Rev. Lett. 13 (1964) 585.
[6] S. Weinberg, Phys. Rev. Lett. 19 (1967) 1264.
[7] A. Salam, Elementary particle physics: relativistic groups and analyticity, in: N. Svartholm (Ed.), Eighth Nobel Symposium, Almquvist and Wiksell, Stockholm, 1968, p. 367.
[8] G. 't Hooft, Nucl. Phys. B 33 (1971) 173.
[9] G. 't Hooft, Nucl. Phys. B 35 (1971) 167.
[10] G. 't Hooft, M.J.G. Veltman, Nucl. Phys. B 44 (1972) 189.
[11] D.J. Gross, F. Wilczek, Phys. Rev. Lett. 30 (1973) 1343.
[12] H.D. Politzer, Phys. Rev. Lett. 30 (1973) 1346.
[13] D. Akimov, et al., COHERENT, Science 357 (2017) 1123, arXiv:1708.01294.
[14] M.G. Aartsen, et al., IceCube, Nature 591 (2021) 220; Erratum: Nature 592 (2021) E11, arXiv:2110.15051.
[15] T. Aaltonen, et al., CDF, Science 376 (2022) 170.
[16] M. Awramik, M. Czakon, A. Freitas, G. Weiglein, Phys. Rev. D 69 (2004) 053006, arXiv:hep-ph/0311148.
[17] S. Schael, et al., ALEPH, DELPHI, L3, OPAL, LEP Electroweak, Phys. Rep. 532 (2013) 119, arXiv:1302.3415.
[18] T.A. Aaltonen, et al., CDF, D0, Phys. Rev. D 88 (2013) 052018, arXiv:1307.7627.
[19] M. Aaboud, et al., ATLAS, Eur. Phys. J. C 78 (2018) 110; Erratum: Eur. Phys. J. C 78 (2018) 898, arXiv:1701.07240.
[20] P.A. Zyla, et al., Particle Data Group, PTEP 2020 (2020) 083C01.
[21] B. Abi, et al., Muon g-2, Phys. Rev. Lett. 126 (2021) 141801, arXiv:2104.03281.
[22] G. Bennett, et al., Muon g-2, Phys. Rev. D 73 (2006) 072003, arXiv:hep-ex/0602035.
[23] H. Brown, et al., Muon g-2, Phys. Rev. Lett. 86 (2001) 2227, arXiv:hep-ex/0102017.
[24] T. Aoyama, et al., Phys. Rep. 887 (2020) 1, arXiv:2006.04822.

---

[25] T. Aoyama, M. Hayakawa, T. Kinoshita, M. Nio, Phys. Rev. Lett. 109 (2012) 111808, arXiv:1205.5370.

[26] T. Aoyama, T. Kinoshita, M. Nio, Atoms 7 (2019) 28.

[27] A. Czarnecki, W.J. Marciano, A. Vainshtein, Phys. Rev. D 67 (2003) 073006; Erratum: Phys. Rev. D 73 (2006) 119901, arXiv:hep-ph/0212229.

[28] C. Gnendiger, D. Stöckinger, H. Stöckinger-Kim, Phys. Rev. D 88 (2013) 053005, arXiv:1306.5546.

[29] M. Davier, A. Hoecker, B. Malaescu, Z. Zhang, Eur. Phys. J. C 77 (2017) 827, arXiv:1706.09436.

[30] A. Keshavarzi, D. Nomura, T. Teubner, Phys. Rev. D 97 (2018) 114025, arXiv:1802.02995.

[31] G. Colangelo, M. Hoferichter, P. Stoffer, J. High Energy Phys. 02 (2019) 006, arXiv:1810.00007.

[32] M. Hoferichter, B.-L. Hoid, B. Kubis, J. High Energy Phys. 08 (2019) 137, arXiv:1907.01556.

[33] M. Davier, A. Hoecker, B. Malaescu, Z. Zhang, Eur. Phys. J. C 80 (2020) 241; Erratum: Eur. Phys. J. C 80 (2020) 410, arXiv:1908.00921.

[34] A. Keshavarzi, D. Nomura, T. Teubner, Phys. Rev. D 101 (2020) 014029, arXiv:1911.00367.

[35] A. Kurz, T. Liu, P. Marquard, M. Steinhauser, Phys. Lett. B 734 (2014) 144, arXiv:1403.6400.

[36] K. Melnikov, A. Vainshtein, Phys. Rev. D 70 (2004) 113006, arXiv:hep-ph/0312226.

[37] P. Masjuan, P. Sanchez-Puertas, Phys. Rev. D 95 (2017) 054026, arXiv:1701.05829.

[38] G. Colangelo, M. Hoferichter, M. Procura, P. Stoffer, J. High Energy Phys. 04 (2017) 161, arXiv:1702.07347.

[39] M. Hoferichter, B.-L. Hoid, B. Kubis, S. Leupold, S.P. Schneider, J. High Energy Phys. 10 (2018) 141, arXiv:1808.04823.

[40] A. Gérardin, H.B. Meyer, A. Nyffeler, Phys. Rev. D 100 (2019) 034520, arXiv:1903.09471.

[41] J. Bijnens, N. Hermansson-Truedsson, A. Rodríguez-Sánchez, Phys. Lett. B 798 (2019) 134994, arXiv:1908.03331.

[42] G. Colangelo, F. Hagelstein, M. Hoferichter, L. Laub, P. Stoffer, J. High Energy Phys. 03 (2020) 101, arXiv:1910.13432.

[43] T. Blum, N. Christ, M. Hayakawa, T. Izubuchi, L. Jin, C. Jung, C. Lehner, Phys. Rev. Lett. 124 (2020) 132002, arXiv:1911.08123.

[44] G. Colangelo, M. Hoferichter, A. Nyffeler, M. Passera, P. Stoffer, Phys. Lett. B 735 (2014) 90, arXiv:1403.7512.

[45] C. Athanassopoulos, et al., LSND, Phys. Rev. C 54 (1996) 2685, arXiv:nucl-ex/9605001.

[46] A. Aguilar-Arevalo, et al., LSND, Phys. Rev. D 64 (2001) 112007, arXiv:hep-ex/0104049.

[47] A.A. Aguilar-Arevalo, et al., MiniBooNE, Phys. Rev. Lett. 102 (2009) 101802, arXiv:0812.2243.

[48] A.A. Aguilar-Arevalo, et al., MiniBooNE, Phys. Rev. Lett. 121 (2018) 221801, arXiv:1805.12028.

[49] A.A. Aguilar-Arevalo, et al., MiniBooNE, Phys. Rev. D 103 (2021) 052002, arXiv:2006.16883.

[50] Y.-Z. Fan, T.-P. Tang, Y.-L.S. Tsai, L. Wu, arXiv:2204.03693, 2022.

[51] C.-R. Zhu, M.-Y. Cui, Z.-Q. Xia, Z.-H. Yu, X. Huang, Q. Yuan, Y.Z. Fan, arXiv:2204.03767, 2022.

[52] C.-T. Lu, L. Wu, Y. Wu, B. Zhu, arXiv:2204.03796, 2022.

[53] B.-Y. Zhu, S. Li, J.-G. Cheng, R.-L. Li, Y.-F. Liang, arXiv:2204.04688, 2022.

[54] H. Song, W. Su, M. Zhang, arXiv:2204.05085, 2022.

[55] H. Bahl, J. Braathen, G. Weiglein, arXiv:2204.05269, 2022.

[56] Y. Heo, D.-W. Jung, J.S. Lee, arXiv:2204.05728, 2022.

[57] K.S. Babu, S. Jana, V.P. K., arXiv:2204.05303, 2022.

[58] T. Biekötter, S. Heinemeyer, G. Weiglein, arXiv:2204.05975, 2022.

[59] Y.H. Ahn, S.K. Kang, R. Ramos, arXiv:2204.06485, 2022.

[60] X.-F. Han, F. Wang, L. Wang, J.M. Yang, Y. Zhang, arXiv:2204.06505, 2022.

[61] G. Arcadi, A. Djouadi, arXiv:2204.08406, 2022.

[62] K. Ghorbani, P. Ghorbani, arXiv:2204.09001, 2022.

[63] J. Kim, S. Lee, P. Sanyal, J. Song, arXiv:2205.01701, 2022.

[64] S. Lee, K. Cheung, J. Kim, C.-T. Lu, J. Song, arXiv:2204.10338, 2022.

[65] O. Atkinson, M. Black, C. Englert, A. Lenz, A. Rusov, arXiv:2207.02789, 2022.

[66] J. Kim, Phys. Lett. B 832 (2022) 137220, arXiv:2205.01437.

[67] J.M. Yang, Y. Zhang, arXiv:2204.04202, 2022.

[68] X.K. Du, Z. Li, F. Wang, Y.K. Zhang, arXiv:2204.04286, 2022.

[69] T.-P. Tang, M. Abdughani, L. Feng, Y.-L.S. Tsai, J. Wu, Y.-Z. Fan, arXiv:2204.04356, 2022.

[70] P. Athron, M. Bach, D.H.J. Jacob, W. Kotlarski, D. Stöckinger, A. Voigt, arXiv:2204.05285, 2022.

[71] M.-D. Zheng, F.-Z. Chen, H.-H. Zhang, arXiv:2204.06541, 2022.

[72] A. Ghoshal, N. Okada, S. Okada, D. Raut, Q. Shafi, A. Thapa, arXiv:2204.07138, 2022.

[73] Y. Cheng, X.-G. He, Z.-L. Huang, M.-W. Li, Phys. Lett. B 831 (2022) 137218, arXiv:2204.05031.

[74] X.K. Du, Z. Li, F. Wang, Y.K. Zhang, arXiv:2204.05760, 2022.

[75] S. Kanemura, K. Yagyu, Phys. Lett. B 831 (2022) 137217, arXiv:2204.07511.

[76] P. Mondal, arXiv:2204.07844, 2022.

[77] D. Borah, S. Mahapatra, D. Nanda, N. Sahu, arXiv:2204.08266, 2022.

[78] G. Senjanović, M. Zantedeschi, arXiv:2205.05022, 2022.

[79] H. Bahl, W.H. Chiu, C. Gao, L.-T. Wang, Y.-M. Zhong, arXiv:2207.04059, 2022.

[80] M. Blennow, P. Coloma, E. Fernández-Martínez, M. González-López, arXiv:2204.04559, 2022.

[81] F. Arias-Aragón, E. Fernández-Martínez, M. González-López, L. Merlo, arXiv:2204.04672, 2022.

[82] X. Liu, S.-Y. Guo, B. Zhu, Y. Li, arXiv:2204.04834, 2022.

[83] T.A. Chowdhury, J. Heeck, S. Saad, A. Thapa, arXiv:2204.08390, 2022.

[84] O. Popov, R. Srivastava, arXiv:2204.08568, 2022.

[85] A. Batra, S.K. A, S. Mandal, H. Prajapati, R. Srivastava, arXiv:2204.11945, 2022.

[86] P. Athron, A. Fowlie, C.-T. Lu, L. Wu, Y. Wu, B. Zhu, arXiv:2204.03996, 2022.

[87] K. Cheung, W.-Y. Keung, P.-Y. Tseng, arXiv:2204.05942, 2022.

[88] A. Bhaskar, A.A. Madathil, T. Mandal, S. Mitra, arXiv:2204.09031, 2022.

[89] T.A. Chowdhury, S. Saad, arXiv:2205.03917, 2022.

[90] J. de Blas, M. Pierini, L. Reina, L. Silvestrini, arXiv:2204.04204, 2022.

[91] J. Fan, L. Li, T. Liu, K.-F. Lyu, arXiv:2204.04805, 2022.

[92] E. Bagnaschi, J. Ellis, M. Madigan, K. Mimasu, V. Sanz, T. You, arXiv:2204.05260, 2022.

[93] A. Paul, M. Valli, arXiv:2204.05267, 2022.

[94] J. Gu, Z. Liu, T. Ma, J. Shu, arXiv:2204.05296, 2022.

[95] L. Di Luzio, R. Gröber, P. Paradisi, Phys. Lett. B 832 (2022) 137250, arXiv:2204.05284.

[96] M. Endo, S. Mishima, arXiv:2204.05965, 2022.

[97] R. Balkin, E. Madge, T. Menzo, G. Perez, Y. Soreq, J. Zupan, J. High Energy Phys. 05 (2022) 133, arXiv:2204.05992.

[98] V. Cirigliano, W. Dekens, J. de Vries, E. Mereghetti, T. Tong, arXiv:2204.08440, 2022.

[99] D. Borah, S. Mahapatra, N. Sahu, Phys. Lett. B 831 (2022) 137196, arXiv:2204.09671.

[100] H.M. Lee, K. Yamashita, arXiv:2204.05024, 2022.

[101] J. Kawamura, S. Okawa, Y. Omura, arXiv:2204.07022, 2022.

[102] A. Crivellin, M. Kirk, T. Kitahara, F. Mescia, arXiv:2204.05962, 2022.

[103] K.I. Nagao, T. Nomura, H. Okada, arXiv:2204.07411, 2022.

[104] J. Cao, L. Meng, L. Shang, S. Wang, B. Yang, arXiv:2204.09477, 2022.

[105] M.T. Frandsen, M. Rosenlyst, arXiv:2207.01465, 2022.

[106] G.-W. Yuan, L. Zu, L. Feng, Y.-F. Cai, Y.-Z. Fan, arXiv:2204.04183, 2022.

[107] A. Strumia, arXiv:2204.04191, 2022.

[108] G. Cacciapaglia, F. Sannino, Phys. Lett. B 832 (2022) 137232, arXiv:2204.04514.

[109] K. Sakurai, F. Takahashi, W. Yin, arXiv:2204.04770, 2022.

[110] J.J. Heckman, arXiv:2204.05302, 2022.

[111] N.V. Krasnikov, arXiv:2204.06327, 2022.

[112] Z. Péli, Z. Trócsányi, arXiv:2204.07100, 2022.

[113] P. Fileviez Perez, H.H. Patel, A.D. Plascencia, arXiv:2204.07144, 2022.

[114] R.A. Wilson, arXiv:2204.07970, 2022.

[115] K.-Y. Zhang, W.-Z. Feng, arXiv:2204.08067, 2022.

[116] L.M. Carpenter, T. Murphy, M.J. Smylie, arXiv:2204.08546, 2022.

[117] M. Du, Z. Liu, P. Nath, arXiv:2204.09024, 2022.

[118] P. Athron, C. Balázs, D.H.J. Jacob, W. Kotlarski, D. Stöckinger, H. Stöckinger-Kim, J. High Energy Phys. 09 (2021) 080, arXiv:2104.03691.

[119] A. Crivellin, M. Hoferichter, PoS ALPS2019 (2020) 009, arXiv:1905.03789.

[120] C. Athanassopoulos, et al., LSND, Nucl. Instrum. Methods A 388 (1997) 149, arXiv:nucl-ex/9605002.

[121] T. Katori, MiniBooNE, in: 3rd World Summit on Exploring the Dark Side of the Universe, 2020, pp. 139–148, arXiv:2010.06015.

[122] B. Dasgupta, J. Kopp, Phys. Rep. 928 (2021) 63, arXiv:2106.05913.

[123] V. Brdar, J. Kopp, arXiv:2109.08157, 2021.

[124] L. Alvarez-Ruso, E. Saul-Sala, arXiv:2111.02504, 2021.

[125] P. Abratenko, et al., MicroBooNE, arXiv:2110.00409, 2021.

[126] W. Abdallah, R. Gandhi, S. Roy, J. High Energy Phys. 06 (2022) 160, arXiv:2202.09373.

[127] W. Abdallah, R. Gandhi, S. Roy, J. High Energy Phys. 12 (2020) 188, arXiv:2006.01948.

[128] W. Abdallah, R. Gandhi, S. Roy, Phys. Rev. D 104 (2021) 055028, arXiv:2010.06159.

[129] D. London, J. Matias, arXiv:2110.13270, 2021.

[130] M. Blanke, in: 10th Large Hadron Collider Physics Conference, 2022, arXiv:2207.07354.

[131] M. Blanke, S. Iguro, H. Zhang, J. High Energy Phys. 06 (2022) 043, arXiv:2202.10468.

[132] S. Iguro, Phys. Rev. D 105 (2022) 095011, arXiv:2201.06565.

[133] R. Watanabe, arXiv:2207.13544, 2022.

[134] T. Lee, Phys. Rev. D 8 (1973) 1226.

[135] G. Branco, P. Ferreira, L. Lavoura, M. Rebelo, M. Sher, J.P. Silva, Phys. Rep. 516 (2012) 1, arXiv:1106.0034.

[136] G.C. Branco, L. Lavoura, J.P. Silva, CP Violation, vol. 103, 1999.

[137] S. Davidson, H.E. Haber, Phys. Rev. D 72 (2005) 035004; Erratum: Phys. Rev. D 72 (2005) 099902, arXiv:hep-ph/0504050.

[138] W.F.L. Hollik, Fortschr. Phys. 38 (1990) 165.

[139] M.E. Peskin, T. Takeuchi, Phys. Rev. D 46 (1992) 381.
[140] D. Lopez-Val, J. Sola, Eur. Phys. J. C 73 (2013) 2393, arXiv:1211.0311.
[141] J.M. Frere, J.A.M. Vermaseren, Z. Phys. C 19 (1983) 63.
[142] J.A. Grifols, J. Sola, Phys. Lett. B 137 (1984) 257.
[143] J.A. Grifols, J. Sola, Nucl. Phys. B 253 (1985) 47.
[144] S. Bertolini, Nucl. Phys. B 272 (1986) 77.
[145] W. Hollik, Z. Phys. C 32 (1986) 291.
[146] W. Hollik, Z. Phys. C 37 (1988) 569.
[147] A. Denner, R.J. Guth, W. Hollik, J.H. Kuhn, Z. Phys. C 51 (1991) 695.
[148] C.D. Froggatt, R.G. Moorhouse, I.G. Knowles, Phys. Rev. D 45 (1992) 2471.
[149] D. Garcia, J. Sola, Mod. Phys. Lett. A 9 (1994) 211.
[150] P.H. Chankowski, M. Krawczyk, J. Zochowski, Eur. Phys. J. C 11 (1999) 661, arXiv:hep-ph/9905436.
[151] W. Grimus, L. Lavoura, O. Ogreid, P. Osland, J. Phys. G 35 (2008) 075001, arXiv:0711.4022.
[152] W. Grimus, L. Lavoura, O.M. Ogreid, P. Osland, Nucl. Phys. B 801 (2008) 81, arXiv:0802.4353.
[153] A. Broggio, E.J. Chun, M. Passera, K.M. Patel, S.K. Vempati, J. High Energy Phys. 11 (2014) 058, arXiv:1409.3199.
[154] S. Hessenberger, W. Hollik, Eur. Phys. J. C 77 (2017) 178, arXiv:1607.04610.
[155] S. Hessenberger, Ph.D. thesis, Munich, Tech. U., 2018.
[156] D. Eriksson, J. Rathsman, O. Stal, Comput. Phys. Commun. 181 (2010) 189, arXiv:0902.0851.
[157] M.J. Dugan, L. Randall, Phys. Lett. B 264 (1991) 154.
[158] R. Barbieri, L.J. Hall, V.S. Rychkov, Phys. Rev. D 74 (2006) 015007, arXiv:hep-ph/0603188.
[159] S. Schael, et al., ALEPH, DELPHI, L3, OPAL, SLD, LEP Electroweak Working Group, SLD Electroweak Group, SLD Heavy Flavour Group, Phys. Rep. 427 (2006) 257, arXiv:hep-ex/0509008.
[160] R. Benbrik, M. Boukidi, B. Manaut, arXiv:2204.11755, 2022.
[161] H. Abouabid, A. Arhrib, R. Benbrik, M. Krab, M. Ouchemhou, arXiv:2204.12018, 2022.
[162] F.J. Botella, F. Cornet-Gomez, C. Miró, M. Nebot, arXiv:2205.01115, 2022.
[163] S. Jana, V.P. K., S. Saad, Phys. Rev. D 101 (2020) 115037, arXiv:2003.03386.
[164] S. Kanemura, T. Kubota, E. Takasugi, Phys. Lett. B 313 (1993) 155, arXiv:hep-ph/9303263.
[165] I.P. Ivanov, Phys. Rev. D 75 (2007) 035001; Erratum: Phys. Rev. D 76 (2007) 039902, arXiv:hep-ph/0609018.
[166] A. Barroso, P.M. Ferreira, I.P. Ivanov, R. Santos, J. High Energy Phys. 06 (2013) 045, arXiv:1303.5098.
[167] B.W. Lee, C. Quigg, H.B. Thacker, Phys. Rev. D 16 (1977) 1519.
[168] A.G. Akeroyd, A. Arhrib, E.-M. Naimi, Phys. Lett. B 490 (2000) 119, arXiv:hep-ph/0006035.
[169] B. Grinstein, C.W. Murphy, P. Uttayarat, J. High Energy Phys. 06 (2016) 070, arXiv:1512.04567.
[170] V. Cacchio, D. Chowdhury, O. Eberhardt, C.W. Murphy, J. High Energy Phys. 11 (2016) 026, arXiv:1609.01290.
[171] S. Chang, S.K. Kang, J.-P. Lee, J. Song, Phys. Rev. D 92 (2015) 075023, arXiv:1507.03618.
[172] M. Aaboud, et al., ATLAS, Phys. Rev. D 98 (2018) 052003, arXiv:1807.08639.
[173] M. Aaboud, et al., ATLAS, Phys. Lett. B 789 (2019) 508, arXiv:1808.09054.
[174] M. Aaboud, et al., ATLAS, Phys. Rev. D 99 (2019) 072001, arXiv:1811.08856.
[175] G. Aad, et al., ATLAS, Eur. Phys. J. C 80 (2020) 957; Erratum: Eur. Phys. J. C 81 (2021) 29; Erratum: Eur. Phys. J. C 81 (2021) 398, arXiv:2004.03447.
[176] A.M. Sirunyan, et al., CMS, J. High Energy Phys. 03 (2019) 026, arXiv:1804.03682.
[177] A.M. Sirunyan, et al., CMS, Phys. Rev. Lett. 122 (2019) 021801, arXiv:1807.06325.
[178] S. Hessenberger, W. Hollik, arXiv:2207.03845, 2022.
[179] M.W. Winkler, Phys. Rev. D 99 (2019) 015018, https://doi.org/10.1103/PhysRevD.99.015018.
[180] R. Acciarri, et al., MicroBooNE, J. Instrum. 12 (2017) P02017, arXiv:1612.05824.
[181] P. Abratenko, et al., MicroBooNE, arXiv:2110.13978, 2021.
[182] P. Abratenko, et al., MicroBooNE, Phys. Rev. Lett. 128 (2022) 241801, arXiv:2110.14054.
[183] P. Abratenko, et al., MicroBooNE, Phys. Rev. D 105 (2022) 112004, arXiv:2110.14065.
[184] P. Abratenko, et al., MicroBooNE, Phys. Rev. D 105 (2022) 112003, arXiv:2110.14080.
[185] M. Antonello, et al., MicroBooNE, LAr1-ND, ICARUS-WA104, arXiv:1503.01520, 2015.
[186] E.M. Riordan, et al., Phys. Rev. Lett. 59 (1987) 755.
[187] J. Lees, et al., BaBar, Phys. Rev. Lett. 113 (2014) 201801, arXiv:1406.2980.
[188] M. Battaglieri, et al., Nucl. Instrum. Methods A 777 (2015) 91, arXiv:1406.6115.
[189] B. Batell, A. Freitas, A. Ismail, D. Mckeen, Phys. Rev. D 98 (2018) 055026, arXiv:1712.10022.
[190] B. Abi, et al., DUNE, Eur. Phys. J. C 81 (2021) 322, arXiv:2008.12769.
[191] P. Ballett, T. Boschi, S. Pascoli, J. High Energy Phys. 03 (2020) 111, arXiv:1905.00284.
[192] C.A. Argüelles, et al., Rep. Prog. Phys. 83 (2020) 124201, arXiv:1907.08311.
[193] J.M. Berryman, A. de Gouvea, P.J. Fox, B.J. Kayser, K.J. Kelly, J.L. Raaf, J. High Energy Phys. 02 (2020) 174, arXiv:1912.07622.
[194] A.M. Sirunyan, et al., CMS, Eur. Phys. J. C 80 (2020) 75, arXiv:1908.06463.